J|A|C|S COMMUNICATIONS

Published on Web 07/12/2010

Highly Stable and CO-Tolerant $Pt/Ti_{0.7}W_{0.3}O_2$ Electrocatalyst for Proton-Exchange Membrane Fuel Cells

Deli Wang, Chinmayee V. Subban, Hongsen Wang, Eric Rus, Francis J. DiSalvo, and Hector D. Abruña*

Department of Chemistry and Chemical Biology, Cornell University, Ithaca, New York 14853

Received April 21, 2010; E-mail: hda1@cornell.edu

Abstract: The current materials used in proton-exchange membrane fuel cells (PEMFCs) are not sufficiently durable for commercial deployment. One of the major challenges lies in the development of an inexpensive, efficient, and CO-tolerant anode catalyst. Here we report the unique CO-tolerant property of Pt nanoparticles supported on $Ti_{0.7}W_{0.3}O_2$. The $Ti_{0.7}W_{0.3}O_2$ nanoparticles (50 nm) were synthesized via a sol−gel process and platinized using an impregnation−reduction technique. Electrochemical studies of $Pt/Ti_{0.7}W_{0.3}O_2$ show unique CO-tolerant electrocatalytic activity for hydrogen oxidation compared to commercial E-TEK PtRu/C catalysts. Differential electrochemical mass spectrometry measurements show the onset potential for CO oxidation on $Pt/Ti_{0.7}W_{0.3}O_2$ to be below 0.1 V (vs RHE). $Pt/Ti_{0.7}W_{0.3}O_2$ is a promising new anode catalyst for PEMFC applications.

Proton exchange membrane fuel cells (PEMFCs) are an attractive alternative to current energy conversion technologies and are being developed for automotive and portable electronics applications due to their high efficiency, near room temperature operation, and zero emissions.[1] However, there are still many challenges to overcome before their commercial deployment, including the development of inexpensive, durable, and efficient catalysts. Although Pt/C is currently the electrocatalyst of choice for hydrogen oxidation, the catalyst surface is easily poisoned, even by low levels of CO (10 ppm), resulting in a significant degradation in performance. The adsorption of CO on the catalyst surface blocks the adsorption and desorption of hydrogen, causing severe anode polarization.[2] Although PtRu catalysts are currently acknowledged as the best anode materials for PEMFCs under impure hydrogen conditions,[3] their CO tolerance is unsatisfactory for practical PEMFCs applications. Furthermore, Ru is neither stable in the alloy, especially at high current densities, nor abundant.[4] Hence, there is a need for anode catalysts that are stable, inexpensive, and resistant to CO poisoning.

Studies by Niedrach et al. have shown the increased CO tolerance of platinized metal oxides, notably those of tungsten.[5] There are numerous studies focused on W-based, CO-tolerant catalysts, either W-modified Pt electrodes[6] (W deposited onto Pt electrode surfaces or alloyed with Pt) or Pt deposited on the surface of WO_3.[3c,7] However, W is easily oxidized at potentials beyond 0.3 V (vs RHE), and WO_3 cannot be used in PEMFCs due to its low electronic conductivity, which derives from the fact that W is in its highest oxidation state.

TiO_2 has been widely used in photovoltaics, water splitting, and gas sensors[8] due to its mechanical and chemical stability in acidic and oxidative environments. Recently, TiO_2 has also been used as a catalyst support in fuel cells[9] due to its stability, even though its electronic conductivity is much lower than that of conventional carbon supports.[10] The conductivity of pure titania, a large band gap (>3 eV) semiconductor, can be improved by aleovalent cation substitution.

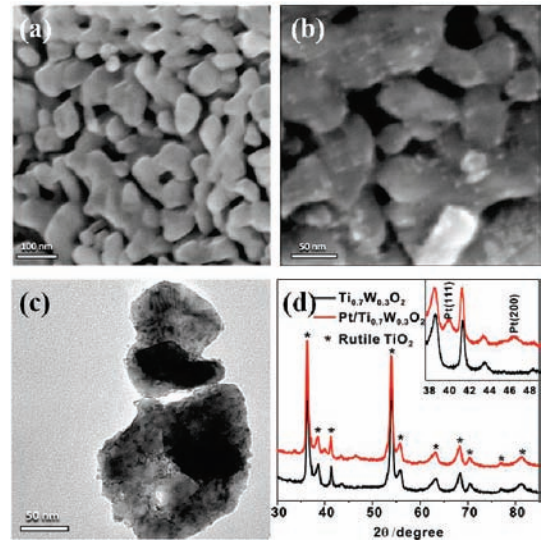

Figure 1. (a) SEM image of $Ti_{0.7}W_{0.3}O_2$. (b) SEM image of $Pt/Ti_{0.7}W_{0.3}O_2$. (c) TEM image of $Pt/Ti_{0.7}W_{0.3}O_2$. (d) XRD patterns of $Ti_{0.7}W_{0.3}O_2$ (black) and $Pt/Ti_{0.7}W_{0.3}O_2$ (red). The inset of (d) shows the enlarged region of Pt (111) and (200) diffraction peaks.

Here we describe the synthesis and characterization of nanoparticles of Pt supported on conducting $Ti_{0.7}W_{0.3}O_2$ and their unique CO-tolerant electrocatalytic activity. $Ti_{0.7}W_{0.3}O_2$ nanoparticles were synthesized via a sol−gel-based multistep synthesis involving *in situ* polymerization of citric acid and ethylene glycol. The air-calcined product with W^{VI} was reduced to W^{IV} by heating to 750 °C with stoichiometric amounts of Zr foil in a sealed, evacuated silica tube.[11] Nanoparticles of Pt were deposited on the oxide by impregnating $Ti_{0.7}W_{0.3}O_2$ nanoparticles in a warm solution of H_2PtCl_6, sonicating, drying, and finally reducing with forming gas.

Figure 1 shows SEM images of $Ti_{0.7}W_{0.3}O_2$ particles (20−50 nm) before (a) and after deposition of 5 wt % Pt (b). The Pt nanoparticles are the bright spots distributed on the surface of the oxide. The uniform distribution of the Pt nanoparticles was verified through elemental mapping using SEM-EDX (Figure S1, Supporting Information) as well as via TEM imaging (Figure 1c). The presence of Pt was further confirmed through XRD (Figure 1d). The diffraction peaks of $Ti_{0.7}W_{0.3}O_2$ could be completely indexed to a tetragonal unit cell, shifted slightly from that of pure rutile-TiO_2 due to W doping. The formation of crystalline Pt nanoparticles was confirmed by the Pt (111) reflection ($2\theta \approx 40°$). The low intensity of the Pt peaks is ascribed to low Pt loading and small particle size.

10.1021/ja102931d

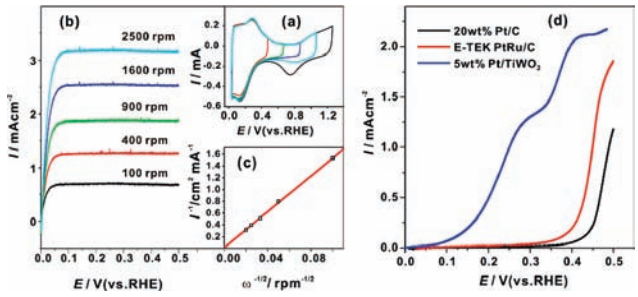

Figure 2. (a) CV at 50 mV s^{-1} of $Pt/Ti_{0.7}W_{0.3}O_2$ (with 20 wt % C added) at different positive potentials limits in 0.1 M H_2SO_4 purged with N_2. (b) H_2 oxidation on $Pt/Ti_{0.7}W_{0.3}O_2$ (with 20 wt % C added) RDE (1 mV s^{-1}) in 0.1 M H_2SO_4 saturated with H_2 at various rates of rotation. (c) Levich plot of (b) in the diffusion-limited potential region at 0.25 V. (d) Polarization curves for H_2 oxidation on different catalysts in the presence of 2% CO at room temperature. Rotation rate, 1600 rpm; scan rate, 1 mV s^{-1}.

$Ti_{0.7}W_{0.3}O_2$ nanoparticles were observed to be stable, through both XRD and SEM (Figure S2), when heated at 80 °C in 5 wt % Nafion solution for up to 3 weeks. The electrochemical stability of $Pt/Ti_{0.7}W_{0.3}O_2$ was tested by potential cycling between +0.05 and +1.1 V at 50 mV s^{-1} in 0.1 M H_2SO_4 for 500 cycles (Figure S3, Supporting Information). Initial tests indicate that $Pt/Ti_{0.7}W_{0.3}O_2$ is more stable than Pt/C and PtRu/C catalysts. After 500 cycles, the loss in the integrated Coulombic charge of the CV for $Pt/Ti_{0.7}W_{0.3}O_2$ was only 5%, while it was over 30% in the case of a commercial E-TEK PtRu/C catalyst.

The electrocatalytic activity for H_2 oxidation and CO tolerance of $Pt/Ti_{0.7}W_{0.3}O_2$ nanoparticles were evaluated using rotating disk electrode (RDE) voltammetry (Figure 2). (Sufficient electronic conductivity was ensured by adding 20 wt % VulcanXC72R to the $Pt/Ti_{0.7}W_{0.3}O_2$ to prepare the ink.) The CV profile of $Pt/Ti_{0.7}W_{0.3}O_2$ (Figure 2a) exhibited hydrogen adsorption/desorption as well as oxide formation and reduction peaks characteristic of a polycrystalline platinum electrode. However, the Coulombic charge of the hydrogen region was much larger than that of the oxide, which could be a result of hydrogen spillover from Pt to $Ti_{0.7}W_{0.3}O_2$. The $Pt/Ti_{0.7}W_{0.3}O_2$ electrocatalyst exhibited negligible overpotential for H_2 oxidation, as would be expected for pure Pt nanoparticles (Figure 2b). The Levich plot (Figure 2c) obtained using the results shown in Figure 2b in the diffusion-limited potential region at 0.25 V gives a slope of 8.5×10^{-2} mA cm^{-2} $rpm^{-1/2}$, which is in good agreement with the literature value for Pt/C.[12] The CO tolerance of $Pt/Ti_{0.7}W_{0.3}O_2$ was evaluated by CO stripping in 0.1 M H_2SO_4 at 50 mV s^{-1} (Figure S4, Supporting Information). When compared to Pt/C and PtRu/C catalysts (Figure S4a−c), the most notable feature of CO stripping on the $Pt/Ti_{0.7}W_{0.3}O_2$ electrocatalyst was the relatively negative potential of the "pre-peak" at 0.3 V. Similar results have been reported for both porous Pt electrodes with adsorbed W species and Mo-modified Pt single-crystal electrodes.[6b,13] To distinguish between the currents arising due to CO_{ads} electrooxidation and the electrochemical response of $Ti_{0.7}W_{0.3}O_2$, the CO stripping experiment was repeated in an H_2-saturated solution for all the catalysts (Figure S4a′−c′). The $Pt/Ti_{0.7}W_{0.3}O_2$ catalyst exhibited a large decrease in the H_2 oxidation overpotential. In addition, the polarization curves for H_2 oxidation in the presence of 2% CO for the various catalysts (Pt/C, PtRu/C, and $Pt/Ti_{0.7}W_{0.3}O_2$) exhibited dramatically different responses. As can be seen in Figure 2, $Pt/Ti_{0.7}W_{0.3}O_2$ exhibited the lowest onset potential for H_2 oxidation (ca. 0.05 V vs RHE) relative to both Pt/C and PtRu/C, which exhibited onset potentials that were over 250 mV more positive. Moreover, $Pt/Ti_{0.7}W_{0.3}O_2$ exhibited two plateaus in the voltammetric profile, and upon increasing the rate of rotation,

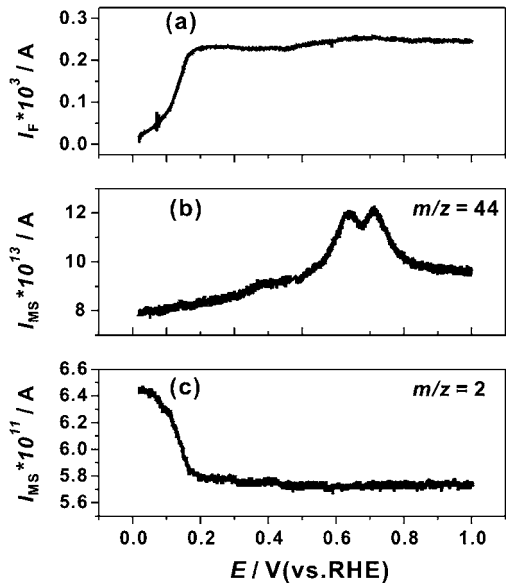

Figure 3. H_2 oxidation on a $Pt/Ti_{0.7}W_{0.3}O_2$ (with 20 wt % C added) thin-film electrode in a thin-layer DEMS flow-cell in the presence of 2% CO in 0.1 M H_2SO_4 at an electrolyte flow rate of 15 μL s^{-1} and a potential scan rate of 1 mV s^{-1}: Faradaic current (a) and corresponding mass spectrometric signals of CO_2 at $m/z = 44$ (b) and H_2 at $m/z = 2$ (c).

the current at the lower potential plateau decreased while that for the higher potential plateau increased (Figure S5, Supporting Information).

Differential electrochemical mass spectrometry (DEMS) measurements were conducted to distinguish the currents of CO oxidation and hydrogen oxidation from that of possible W oxidation (Figure 3). The polarization characteristics of hydrogen oxidation in Figure 3a are similar to the RDE results at low rotation rates (Figure S5, Supporting Information, 400 rpm), and the anodic current starts to increase at about 0.05 V. The concurrent mass spectrometric signal at $m/z = 44$ (Figure 3b) shows that the onset potential for CO_2 formation is below 0.1 V. This lends additional support to our previous assertion that $(Ti/W)O_2$ can significantly cocatalyze CO oxidation. The onset of H_2 oxidation, which is indicated by the decrease in the mass spectrometric signal intensity at $m/z = 2$ (Figure 3c), coincides perfectly with the onset of CO_2 formation. At a solution flow rate of 15 μL/s, the hydrogen oxidation current on $Pt/Ti_{0.7}W_{0.3}O_2$ reached its diffusion-limited value at 0.2 V, even though only a very small fraction of CO is oxidized.

It appears that not only the W in the $Pt/Ti_{0.7}W_{0.3}O_2$ catalyst but also the TiO_2 contribute to the higher activity for CO oxidation on Pt. This may be due to electronic effects from the TiO_2 (Figure S6, Supporting Information). The onset potential of CO oxidation at $Pt/Ti_{0.7}W_{0.3}O_2$ occurs at 0.05 V, and a small pre-peak occurs at a potential of 0.15 V, as shown in the MSCV of CO_2 at $m/z = 44$ (Figure S6a′). In contrast, the pre-peak of CO oxidation at a PtW/C alloy catalyst is more positive than that of the $Pt/Ti_{0.7}W_{0.3}O_2$ catalyst (Figure S6b′). Furthermore, the main peak of CO oxidation on $Pt/Ti_{0.7}W_{0.3}O_2$ is also shifted 100 mV more negative than that of the PtW/C alloy catalyst.

In conclusion, $Ti_{0.7}W_{0.3}O_2$ was successfully synthesized using a sol−gel technique, and platinum nanoparticles were uniformly deposited on the oxide. Chemical and electrochemical studies indicate high stability of both $Ti_{0.7}W_{0.3}O_2$ and $Pt/Ti_{0.7}W_{0.3}O_2$ nanoparticles. $Pt/Ti_{0.7}W_{0.3}O_2$ exhibits high activity for H_2 oxidation as well as a higher CO tolerance than Pt/C and PtRu/C catalysts. $Pt/Ti_{0.7}W_{0.3}O_2$ is a promising anode catalyst for PEMFC applications.

Acknowledgment. This work was supported by the Department of Energy though grant DE-FG02-87ER45298 and by the Energy Materials Center at Cornell, an Energy Frontier Research Center funded by the U.S. Department of Energy, Office of Science, Office of Basic Energy Sciences under Award Number DE-SC0001086. We acknowledge helpful discussions with General Motors Fuel Cell Activities. This work made use of SEM and TEM facilities of the Cornell Center for Materials Research (CCMR).

Supporting Information Available: Details of synthesis, platinization, and chemical and electrochemical stability tests. This material is available free of charge via the Internet at http://pubs.acs.org.

References

(1) (a) Bashyam, R.; Zelenay, P. *Nature* **2006**, *443*, 63. (b) Brumfiel, G. *Nature* **2003**, *422*, 104. (c) Steele, B. C. H.; Heinzel, A. *Nature* **2001**, *414*, 345.
(2) (a) Kawatsu, S. *J. Power Sources* **1998**, *71*, 150. (b) Haug, A. T.; White, R. E.; Weidner, J. W.; Huang, W. *J. Electrochem. Soc.* **2002**, *149*, A862. (c) Wee, J. H.; Lee, K. Y. *J. Power Sources* **2006**, *157*, 128.
(3) (a) Schmidt, T. J.; Noeske, M.; Gasteiger, H. A.; Behm, R. J.; Britz, P.; Brijoux, W.; Bonnemann, H. *Langmuir* **1997**, *13*, 2591. (b) Kabbabi, A.; Faure, R.; Durand, R.; Beden, B.; Hahn, F.; Leger, J. M.; Lamy, C. *J. Electroanal. Chem.* **1998**, *444*, 41. (c) Pereira, L. G. S.; dos Santos, F. R.; Pereira, M. E.; Paganin, V. A.; Ticianelli, E. A. *Electrochim. Acta* **2006**, *51*, 4061. (d) Gasteiger, H. A.; Markovic, N. M.; Ross, P. N. *J. Phys. Chem.* **1995**, *99*, 16757.
(4) Ioroi, T.; Fujiwara, N.; Siroma, Z.; Yasuda, K.; Miyazaki, Y. *Electrochem. Commun.* **2002**, *4*, 442.
(5) Niedrach, L. W.; Weinstoc, I. B. *Electrochem.Tech.* **1965**, *3*, 270.
(6) (a) Pereira, L. G. S.; Paganin, V. A.; Ticianelli, E. A. *Electrochim. Acta* **2009**, *54*, 1992. (b) Nagel, T.; Bogolowski, N.; Samjeske, G.; Baltruschat, H. *J. Solid State Electrochem.* **2003**, *7*, 614. (c) Colmenares, L.; Jusys, Z.; Kinge, S.; Bonnemann, H.; Behm, R. J. *J. New Mater. Electrochem. Syst.* **2006**, *9*, 107.
(7) (a) Maillard, F.; Peyrelade, E.; Soldo-Olivier, Y.; Chatenet, M.; Chainet, E.; Faure, R. *Electrochim. Acta* **2007**, *52*, 1958. (b) Hobbs, B. S.; Tseung, A. C. C. *Nature* **1969**, *222*, 556. (c) Christian, J. B.; Smith, S. P. E.; Whittingham, M. S.; Abruna, H. D. *Electrochem. Commun.* **2007**, *9*, 2128. (d) Micoud, F.; Maillard, F.; Gourgaud, A.; Chatenet, M. *Electrochem. Commun.* **2009**, *11*, 651. (e) Cui, X. Z.; Guo, L. M.; Cui, F. M.; He, Q. J.; Shi, J. L. *J. Phys. Chem. C* **2009**, *113*, 4134. (f) Chhina, H.; Campbell, S.; Kesler, O. *J. Electrochem. Soc.* **2007**, *154*, B533.
(8) Chen, X.; Mao, S. S. *Chem. Rev.* **2007**, *107*, 2891.
(9) (a) Huang, S. Y.; Ganesan, P.; Park, S.; Popov, B. N. *J. Am. Chem. Soc.* **2009**, *131*, 13898. (b) Selvarani, G.; Maheswari, S.; Sridhar, P.; Pitchumani, S.; Shukla, A. K. *J. Electrochem. Soc.* **2009**, *156*, B1354.
(10) (a) Ioroi, T.; Siroma, Z.; Fujiwara, N.; Yamazaki, S.; Yasuda, K. *Electrochem. Commun.* **2005**, *7*, 183. (b) Chen, J. M.; Sarma, L. S.; Chen, C. H.; Cheng, M. Y.; Shih, S. C.; Wang, G. R.; Liu, D. G.; Lee, J. F.; Tang, M. T.; Hwang, B. J. *J. Power Sources* **2006**, *159*, 29.
(11) Marezio, M.; Bordet, P.; Capponi, J. J.; Cava, R. J.; Chaillout, C.; Chenavas, J.; Hewat, A. W.; Hewat, E. A.; Hodeau, J. L.; Strobel, P. *Physica C* **1989**, *162*, 281.
(12) Schmidt, T. J.; Jusys, Z.; Gasteiger, H. A.; Behm, R. J.; Endruschat, U.; Boennemann, H. *J. Electroanal. Chem.* **2001**, *501*, 132.
(13) (a) Massong, H.; Wang, H. S.; Samjeske, G.; Baltruschat, H. *Electrochim. Acta* **2000**, *46*, 701. (b) Samjeske, G.; Wang, H. S.; Loffler, T.; Baltruschat, H. *Electrochim. Acta* **2002**, *47*, 3681.

JA102931D